Eur. Phys. J. C 34, 41–49 (2004)
Digital Object Identifier (DOI) 10.1140/epjc/s2004-01765-9

THE EUROPEAN
PHYSICAL JOURNAL C

W & Z physics at LEP

P. Zerwas

DESY, Notkestr. 85, 22607 Hamburg, Germany

Received: 15 December 2003 /
Published online: 4 May 2004 –

1 Introduction

The fundamental laws of nature which govern the microscopic world have been systematically explored by particle physics since the middle of the last century. Particle physics has succeeded not only in revealing the structure of matter, but also in explaining its interactions. The present state of our knowledge is contained in the Standard Model, formulated at the quantum level as required for microscopic physics. The model incorporates three components: the matter particles are grouped in three lepton and quark families; the forces are generated by the electromagnetic, weak and strong interactions; and the Higgs mechanism, still hypothetical, is introduced to generate the masses of the fundamental particles[1]. Gravity is attached *ad hoc* as a classical phenomenon but not deeply incorporated into the system.

The electromagnetic and weak interactions are unified to electroweak interactions within the Standard Model – one of the greatest achievements of physics in the 20th century. They are formulated in the Glashow–Salam–Weinberg model [1, 2] as an SU(2) × U(1) gauge field theory, including the Higgs mechanism for generating the masses [3].

The first two crucial steps in establishing the electroweak part of the Standard Model experimentally were the discovery of Neutral Currents in neutrino scattering by the Gargamelle Collaboration [4, 5] and, only a decade later, the discovery of the gauge bosons $W^\pm$ and Z in $\bar{p}p$ collisions at the $S\bar{p}pS$ collider by the UA1 and UA2 Collaborations [6, 7].

Establishing the theory at the quantum level was the next logical experimental step. This step followed the pioneering theoretical work by G. 't Hooft and M. Veltman [8] by which the renormalizibility of the Standard Model, as a non-Abelian/Abelian massive gauge field theory incorporating the Higgs mechanism, was proven, *i.e.* the firm mathematical foundation and basis for precise calculations of physical quantities. The theory could be extended from leptons to hadrons after the charm quark was introduced by the Glashow–Iliopoulos–Maiani mechanism [9].

Peter Zerwas

The experimental proof that the theory correctly describes phenomena at the quantum level is a necessary requirement for any theory operating in the microscopic world. At the same time, performing experimental analyses with high precision opens windows to new physics phenomena at high energy scales that can only be accessed indirectly through virtual effects. These goals have been achieved by LEP.

For the fourth step in this process, establishing the Higgs mechanism for generating the masses of the fundamental particles, indirect evidence has been accumulated by LEP but the picture could not be completed. The final decision, most likely, has to await experimentation in the near future at LHC [10].

[1] The observation of non-zero neutrino masses leads to an extension of the Standard Model as conceived originally. While the lepton and quark sectors are symmetrized beautifully by introducing right-handed degrees of freedom for neutrinos, the R-neutrino fields may carry along a new mass parameter generated at high energy scales close to the grand unification scale of the three gauge interactions.

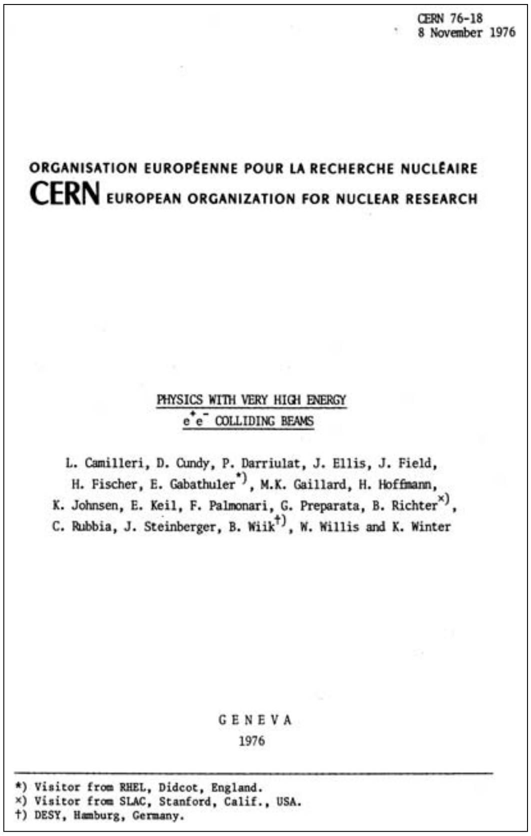

CERN 76-18
8 November 1976

ORGANISATION EUROPÉENNE POUR LA RECHERCHE NUCLÉAIRE
CERN EUROPEAN ORGANIZATION FOR NUCLEAR RESEARCH

PHYSICS WITH VERY HIGH ENERGY
e^+e^- COLLIDING BEAMS

L. Camilleri, D. Cundy, P. Darriulat, J. Ellis, J. Field, H. Fischer, E. Gabathuler*), M.K. Gaillard, H. Hoffmann, K. Johnsen, E. Keil, F. Palmonari, G. Preparata, B. Richter×), C. Rubbia, J. Steinberger, B. Wiik†), W. Willis and K. Winter

GENEVA
1976

*) Visitor from RHEL, Didcot, England.
×) Visitor from SLAC, Stanford, Calif., USA.
†) DESY, Hamburg, Germany.

Fig. 1. *left*: cover page of the seminal CERN Report 76-18 [12] on the physics potential of a 200 GeV e^+e^- collider; *right*: LEP at CERN, including the four universal detectors, ALEPH, DELPHI, L3 and OPAL

Before LEP operations started in 1989, the state of the electroweak sector could be described in condensed form by a small set of characteristic parameters, see [11]: the masses of the $W^\pm$ and Z bosons had been measured to an accuracy of a few hundred MeV, and the electroweak mixing angle, $\sin^2\theta_\mathrm{W}$, had been determined at the percent level. The accuracy with which these observables could be measured, led to a prediction of the top-quark mass at 130 ± 50 GeV, but no bound could be derived on the Higgs mass.

Soon after the highly successful operation of e^+e^- colliders in the early 1970's, the idea of building such a facility in the energy region up to 200 GeV was advanced by a group of experimentalists and theorists in a seminal CERN report, CERN 76-18 [1976], in which the physics potential was outlined quite comprehensively [12] (Fig. 1, *left*).

LEP, the Large Electron–Positron Collider (Fig. 1, *right*), finally started operation in 1989, equipped with four universal detectors, ALEPH, DELPHI, L3 and OPAL (Fig. 2). The machine operated in two phases. In the first phase, between 1989 and 1995, 18 million Z bosons were accumulated, while in the second phase, from 1996 to 2000, some 80 thousand W bosons were generated at energies gradually climbing from the W^+W^--pair threshold to the maximum of 209 GeV – with excellent machine performance at all energy steps.

2 Z-Boson physics

2.1 The electroweak basis

The Z boson in the Glashow–Salam–Weinberg model is a mixture of the neutral SU(2) isospin W^3 and the U(1) hypercharge B gauge fields, with the mixing parameterized by the angle θ_W:

$$A = B\cos\theta_\mathrm{W} + W^3\sin\theta_\mathrm{W}$$
$$Z = -B\sin\theta_\mathrm{W} + W^3\cos\theta_\mathrm{W}$$

The Z-boson interacts with vector and axial-vector currents of matter proportional to the Z-charges of the leptons and quarks which are determined by the isospin and the electric charges of the particles:

$$g_V^f = I_{3\mathrm{L}}^f - 2Q'\sin^2\theta_\mathrm{W}$$
$$g_A^f = I_{3\mathrm{L}}^f$$

The Z–matter couplings are affected by electroweak radiative loop corrections. The overall couplings are modified by the ρ parameter while the mixing angle is generically parameterized by the effective value for the lepton currents. High-precision analyses of the couplings therefore allow tests of the theory at the quantum level.

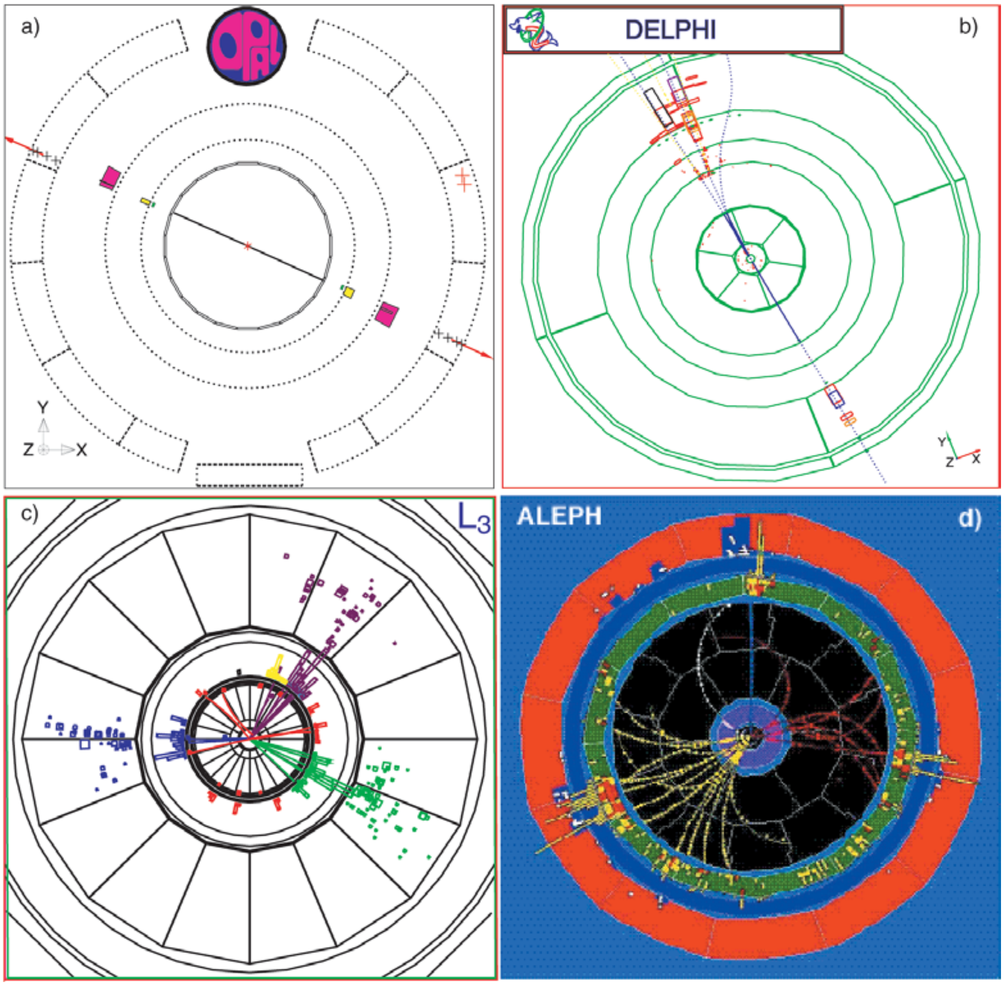

Fig. 2. Typical events, as recorded by the four LEP experiments, **a** $\mu^+\mu^-$ pair in OPAL; **b** $\tau^+\tau^-$ pair in DELPHI; **c** 3-jet event in L3; **d** W^+W^- event close to threshold, with W decays to τ–ν_τ and a pair of jets in ALEPH

The properties of the Z-boson and of the underlying electroweak theory could be studied at LEP by measuring a threefold ensemble of observables: the overall formation cross section, *i.e.* the line-shape, that is parameterized in the Breit–Wigner form by the Z-boson mass and its width; the forward–backward asymmetries of the leptons and quarks; and the polarization of τ leptons, both measuring the vector- and axial-vector Z-boson charges of the fermions involved. Outstandingly clear events could be observed in each of the four detectors (Fig. 2). As a result, the experimental analysis of the Z line-shape (Fig. 3), of the decay branching ratios and the asymmetries could be performed with precision unprecedented in high-energy experiments [13]:

$$M_Z = 91\,187.5 \pm 2.1 \text{ MeV}$$
$$\Gamma_Z = 2495.2 \pm 2.3 \text{ MeV}$$
$$\sin^2\theta_{\text{eff}}^{\text{lept.}} = 0.22138 \pm 0.00014$$

(including SLC results). Thus, the electroweak sector of the Standard Model has passed examination successfully at the per-mille level. This is highlighted by the global analyses of the electroweak mixing parameter $\sin^2\theta_{\text{eff}}^{\text{lept.}}$ – truly in the realm where quantum theory is the proper

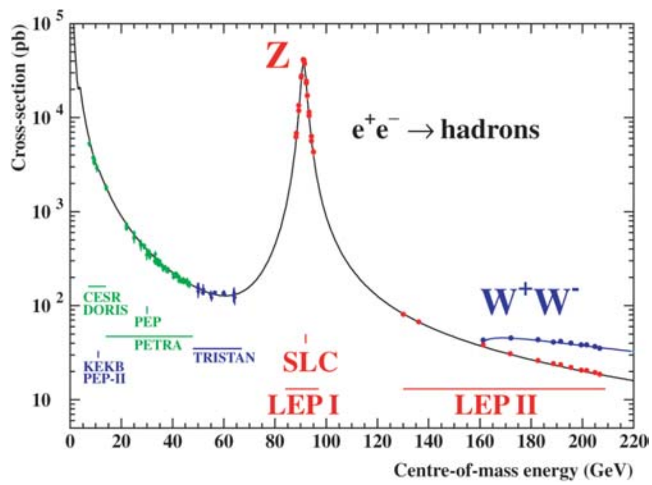

Fig. 3. The e^+e^- annihilation cross section to hadrons, from initial low energies in early colliders to the maximum energy at LEP [13]

basis for formulating the laws of nature. The collection of observables and parameters in Fig. 4 evidently conforms to the theory, with deviations from the average line at the 2 standard deviation level only in the forward–backward asymmetry of b-quark jets and the left–right electron polarization asymmetry measured at the Stanford Linear Collider SLC facility.

Beyond the most stringent test of the electroweak theory itself, important conclusions could be drawn on other aspects of the Standard Model and potential physics beyond by studying the e^+e^- collisions on the tip of the Z-boson resonance and in its Breit–Wigner wings.

2.2 Top-quark prediction

The physics of the top quark has truly been a success story at LEP, even though the particle is too heavy to be produced at a 200 GeV collider. Not only could the existence of this heaviest of all quarks in the Standard Model be predicted, but also its mass could be pre-determined from the analysis of quantum corrections with amazing accuracy – a textbook example of the great potential of fruitful cooperation between theory and experiment in high-precision analyses.

	Measurement	Fit
$\Delta\alpha^{(5)}_{had}(m_Z)$	0.02761 ± 0.00036	0.02767
m_Z [GeV]	91.1875 ± 0.0021	91.1875
Γ_Z [GeV]	2.4952 ± 0.0023	2.4960
σ^0_{had} [nb]	41.540 ± 0.037	41.478
R_l	20.767 ± 0.025	20.742
$A^{0,l}_{fb}$	0.01714 ± 0.00095	0.01636
$A_l(P_\tau)$	0.1465 ± 0.0032	0.1477
R_b	0.21638 ± 0.00066	0.21579
R_c	0.1720 ± 0.0030	0.1723
$A^{0,b}_{fb}$	0.0997 ± 0.0016	0.1036
$A^{0,c}_{fb}$	0.0706 ± 0.0035	0.0740
A_b	0.925 ± 0.020	0.935
A_c	0.670 ± 0.026	0.668
A_l(SLD)	0.1513 ± 0.0021	0.1477
$\sin^2\theta^{lept}_{eff}(Q_{fb})$	0.2324 ± 0.0012	0.2314
m_W [GeV]	80.426 ± 0.034	80.385
Γ_W [GeV]	2.139 ± 0.069	2.093
m_t [GeV]	174.3 ± 5.1	174.3
Q_W(Cs)	-72.84 ± 0.46	-72.90

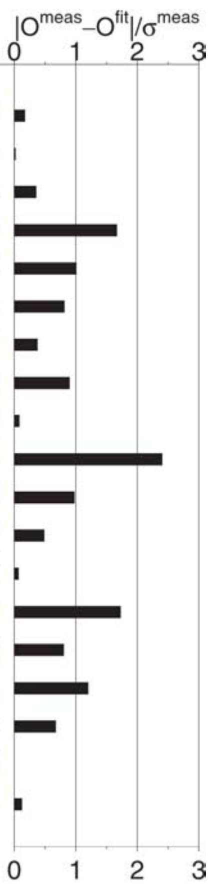

Fig. 4. Precision observables in the electroweak part of the Standard Model, as measured at LEP and elsewhere (excerpt from [13])

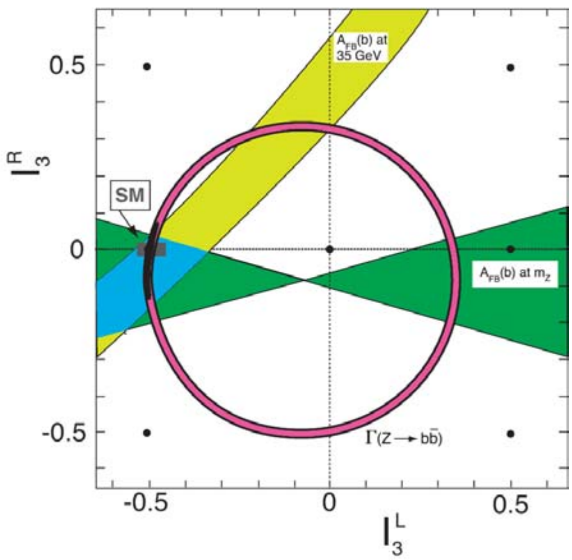

Fig. 5. Determining the weak isospin of the bottom quark [14]; circle: partial Z-decay width to $b\bar{b}$ at LEP; wedges: forward–backward b asymmetry at LEP; strip: $b\bar{b}$ cross section at PETRA. All measurements cross the point $[I_3^L, I_3^R] = [-1/2, 0]$ so that an isospin partner to the b quark with $[I_3^L, I_3^R] = [+1/2, 0]$ should exist – the top quark

By analyzing the partial decay width and the forward–backward asymmetry of Z decays to b-quark jets at LEP and complementing this set by the production rate of b quarks at the lower-energy collider PETRA, which is sensitive to the interference between s-channel γ and Z exchanges, the isospin of the b-quark could be uniquely determined [14] (Fig. 5). From the measured quantum number $I_3^L = -1/2$, the existence of an isospin $+1/2$ partner to the bottom quark could be derived conclusively – the top quark.

More than that: virtual top quarks in $t\bar{b}$ and $t\bar{t}$ loops affect the propagation of the electroweak gauge bosons. This effect modifies, in particular, the relation between the Fermi coupling G_F of β decay, the Z-boson mass M_Z, and the electroweak mixing angle $\sin^2\theta_{eff}^{lept.}$. The correction is parameterized in the ρ parameter and increases quadratically in the top-quark mass [15]:

$$\rho = 1 + \Delta\rho_t + \Delta\rho_H$$
$$\Delta\rho_t \sim +G_F m_t^2$$

leading to the prediction [16]:

$$m_t = 173^{+12+18}_{-13-20}\ \text{GeV}$$

for the top-quark mass before top quarks were established at the Tevatron and the mass confirmed by direct observation.

Truly – a triumph of high-precision experimentation at LEP joined with theoretical high-precision calculations at the quantum level of the Standard Model.

2.3 Quantum chromodynamics QCD

Many of the key elements in QCD, the strong-interaction component [17] of the complete SU(3) × SU(2) × U(1) Standard Model, were established experimentally at e^+e^- colliders. The clean signals make these machines precision instruments for studying QCD, and the observations have contributed significantly towards putting this field theory of the strong interaction on a firm experimental basis.

That quarks come in three colors was indicated quite early on by the ratio of the hadronic e^+e^- annihilation cross section to the μ-pair cross section at ADONE – R being close to the value $3 \times 2/3 = 2$ instead of 2/3 as naively expected in the color-less quark model. While the existence of quark jets was demonstrated a little later at SPEAR, the development was crowned by the observation of the PETRA jets – a direct and clear experimental signal for gluons, the carriers of the microscopic force of the strong interaction. This line continued straight through the LEP experiments.

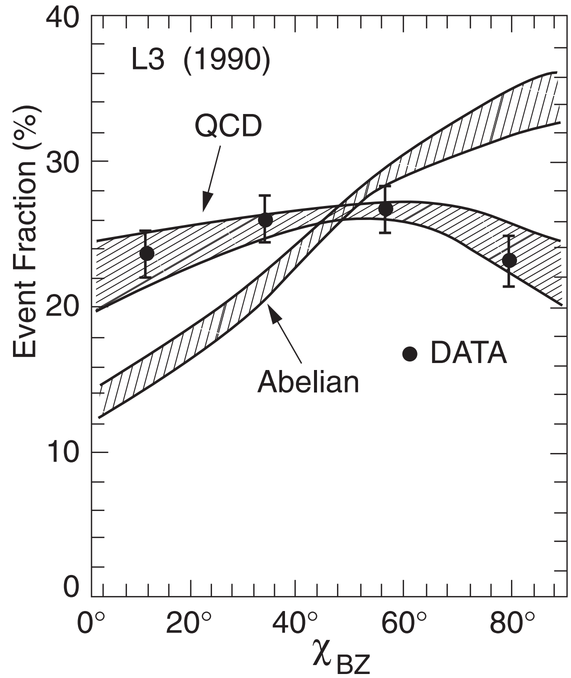

Fig. 7. The distribution of the azimuthal angle between the planes spanned by the high-energy jets and the low-energy jets in 4-jet events of Z decays [21]. The experimental distribution [20] is compatible with QCD, involving the self-coupling of the gluons, but it cannot be reproduced by an Abelian "QED-type" field theory of the strong interaction without gauge-boson self-coupling

2.3.1 QCD coupling

With the measurement of the QCD coupling at the scale M_Z,

$$\alpha_s = 0.1183 \pm 0.0027,$$

and the observation of the running of α_s from low PETRA to high LEP energies as observed in jet analyses [18], the validity of *asymptotic freedom*, a key prediction in QCD [19], was demonstrated in a wonderful way (Fig. 6).

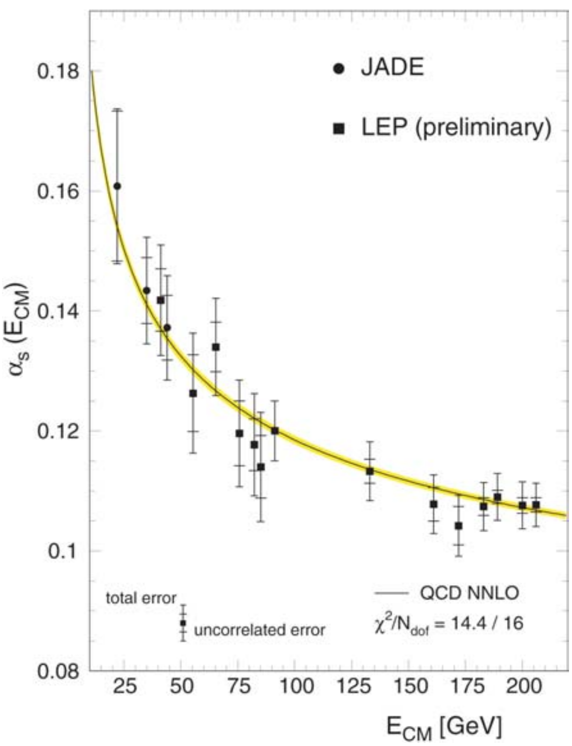

Fig. 6. The running of the QCD coupling from low PETRA to high LEP energies compared with the prediction of asymptotic freedom [18]

2.3.2 Non-Abelian gauge symmetry

With the observation of angular correlations in 4-jet final states of Z-boson decays [20], the 3-gluon self-coupling was clearly established, the characteristic of QCD being a *non-Abelian gauge theory* [21] (Fig. 7). With the measured value of the Casimir invariant [22] C_A,

$$C_A = 3.02 \pm 0.55,$$

the strength of the 3-gluon coupling agrees with the predicted value $C_A = 3$ for non-Abelian SU(3), but being far away from the value zero in any Abelian "QED-type" field theory without self-coupling of the gauge bosons.

2.3.3 Running quark masses

In the same way as couplings run, *quark masses* change when measured at different scales. The change of the mass value is a consequence of the retarded motion of the gluon cloud surrounding the quark when its momentum is altered by absorbing momentum from a hard photon, for instance. This effect could be observed in a unique way by measuring the b-quark mass at the Z scale and comparing

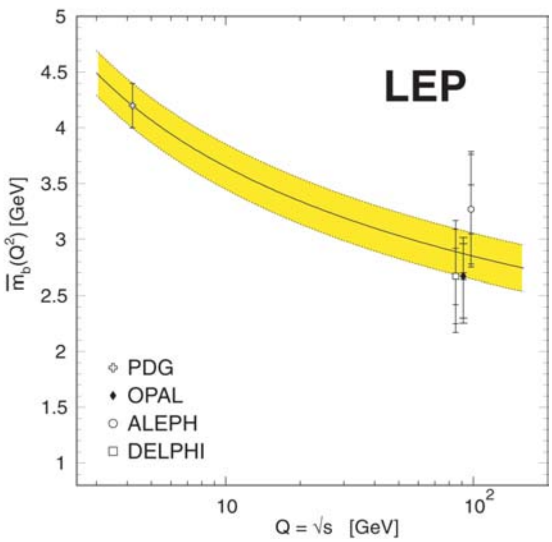

Fig. 8. The change of the bottom-quark mass when weighed at low and at high energies [23]

this value with the value at a low scale [23] (Fig. 8). The measurement of the running b mass agrees well with the prediction of QCD.

2.4 Three families in the Standard Model

The number of light neutrinos was determined at LEP by comparing the Z width as measured in the Breit–Wigner line-shape, with the visible lepton and quark-decay channels [13]. The ensuing difference determines the number of light neutrino species to be three:

$$N_\nu = 2.985 \pm 0.008.$$

Thus, LEP closed the canonical Standard Model with three families of matter particles.

2.5 Gauge coupling unification

When charges are measured in scattering experiments at different values of momentum transfer, they are altered as a consequence of screening and anti-screening effects in gauge field theories. These effects are generated by the vacuum polarization induced by virtual gauge-boson and fermion pairs in the fields surrounding charges. Fermions screen the charges; gauge bosons have the opposite effect, so that couplings in Abelian theories like QED increase when probed for larger momentum transfer, while non-Abelian theories are asymptotically free so long as the number of fermion degrees of freedom is small enough.

Extrapolating the three couplings [24] associated with the gauge symmetries SU(3) × SU(2) × U(1) in the Standard model to increasingly higher scales, they approach each other but do not really meet at the same point. This is different if the particle spectrum of the Standard Model is extended by supersymmetric partners [25] which modify, as virtual particles, the vacuum polarization. Independently of the mass values, so long as they are in the TeV region, the new degrees of freedom make the couplings converge to an accuracy close to 2% [26] (Fig. 9). This observation opens the exciting perspective that the three forces of the Standard Model may be unified at an energy scale close to 2×10^{16} GeV.

At the same time, strong support is given, though indirectly, for supersymmetry – a symmetry intimately related to gravity, the fourth of the fundamental interactions. This may thus lead us closer to the ultimate unification of all the four forces in nature.

Experimental high-precision results from LEP therefore have far-reaching, deep consequences for potential physics scenarios at scales far above the energies directly accessible at accelerators – whatever their energy range may be in even the distant future.

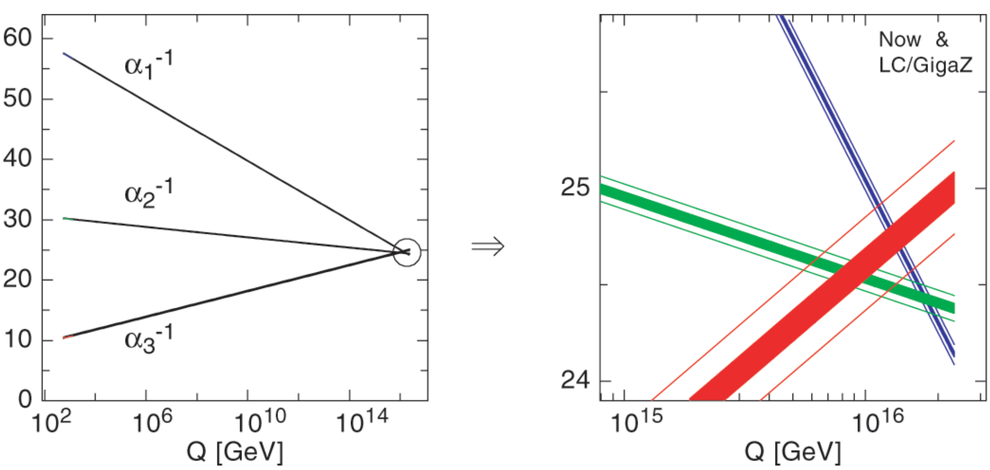

Fig. 9. Extrapolation of the SU(3), SU(2) and U(1) gauge couplings to high energies in the Minimal Supersymmetric extension of the Standard Model. They approach each other near 2×10^{16} GeV at a level of 2%, indicative of the Grand Unification of the three gauge interactions [26]

3 W-Boson physics

Gauge field theories appear to be the theoretical framework within which the three fundamental particle forces can be understood. Introduced by Weyl [27] as the basic symmetry principle of electrodynamics, the scheme was generalized later by Yang and Mills [28] to non-Abelian gauge symmetries before being applied to the electroweak and strong interactions.

One of the central tasks of the LEP experiments at energies beyond the W^+W^--pair threshold was the analysis of the 3-gauge boson couplings, predicted in form and magnitude by the gauge symmetry. A first glimpse could also be caught of the corresponding 4-boson couplings.

Charged W^+W^- pairs are produced in e^+e^- collisions (see Fig. 2) by three different mechanisms – neutrino exchange, and photon- and Z-boson exchanges [29].

From the steep increase of the excitation curve near threshold, and from the reconstruction of the W bosons in both leptonic and hadronic decay modes, the mass $M_{\rm W}$ and the width $\Gamma_{\rm W}$ can be reconstructed with high precision [30]:

$$M_{\rm W} = 80.412 \pm 0.042 \text{ GeV}$$
$$\Gamma_{\rm W} = 2.150 \pm 0.091 \text{ GeV}$$

This value of the directly measured W mass is in excellent agreement with the mass value extracted indirectly from precision observables, as evident from Fig. 10.

Any of the three W^+W^--production mechanisms, if isolated from the others, leads to a cross section that rises indefinitely with energy. However, the amplitudes interfere destructively as predicted by the gauge symmetry between fermion and gauge boson couplings. As a result of these gauge cancellations, the final cross section is damped by

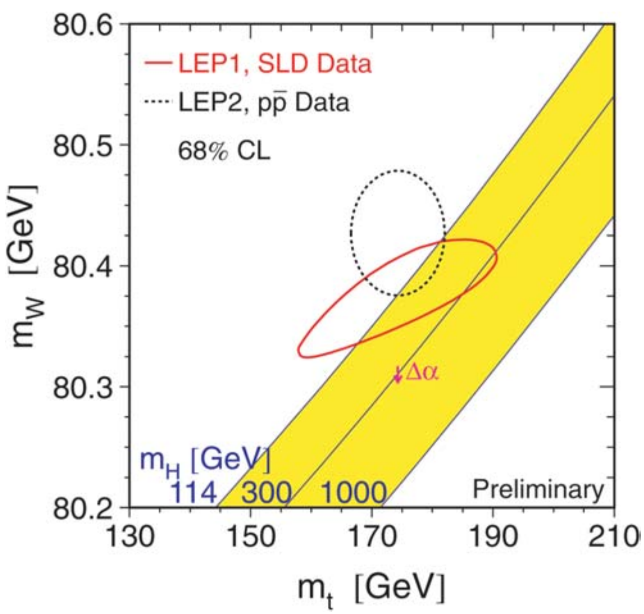

Fig. 10. Comparison of the W-boson and t-quark masses, as extracted from radiative corrections, with the directly measured mass values [13]

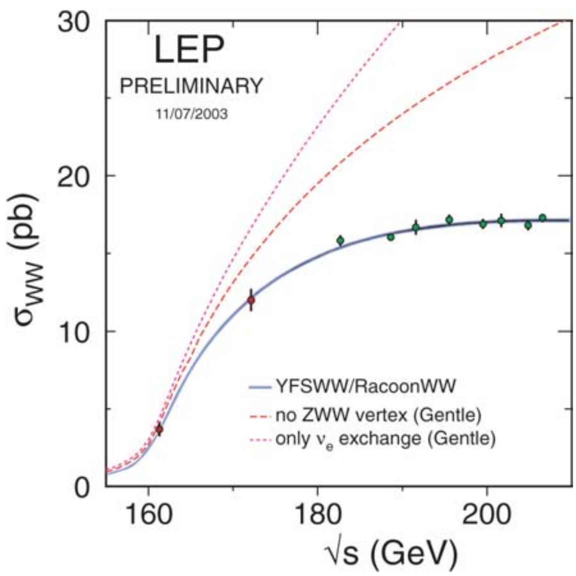

Fig. 11. The total cross section for W-pair production $e^+e^- \to W^+W^-$ at LEP in the Standard Model. The measurements are also confronted with ad-hoc scenarios in which three-boson self-couplings are switched off. The gauge symmetries are evidently crucial for the understanding of the measurements [13]

a factor $1/E^2$ for large energies. The prediction is clearly borne out by the LEP data [13] (Fig. 11), thus confirming the crucial impact of gauge symmetries on the dynamics of the electroweak sector in the Standard Model in a most impressive way.

The impact of the gauge symmetries on the trilinear couplings can be quantified by measuring the static electroweak parameters of the charged W bosons, *i.e.* the monopole charges, the magnetic dipole moments and the electric quadrupole moments of the W bosons coupled to the γ and to the Z boson; for the photon coupling,

$$g_1 = e$$
$$\mu_{\rm W} = 2 \times \frac{e}{2M_{\rm W}}$$
$$q_{\rm W} = -\frac{e}{M_{\rm W}^2}$$

and for the Z coupling analogously. These predictions were confirmed experimentally within a margin of a few percent.

Studying the quartic couplings requires 3-boson final states. Some first analyses of $W^+W^-\gamma$ final states have bounded any anomalies to less than a few percent.

4 Higgs mechanism

The fourth step in establishing the electroweak sector of the Standard Model experimentally, the search for the Higgs particle, could not be completed by LEP. Nevertheless, two important results were reported by the experiments.

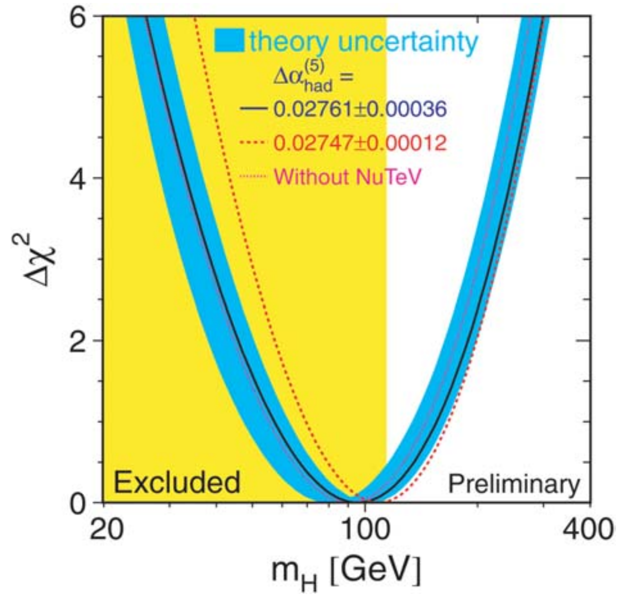

Fig. 12. "Blue-Band Plot": Probability distribution of the Higgs mass in the Standard Model [and related theories], derived from precision data from LEP and elsewhere [13]

4.1 Virtual Higgs mass estimate

By emitting and reabsorbing a virtual Higgs boson from a propagating electroweak boson, the mass of the boson is slightly shifted. In parallel with the top quark, this effect can be included in the ρ parameter. With the contribution [31]

$$\Delta\rho_H \sim -G_F M_W^2 \log M_H^2/M_W^2$$

the Higgs boson is screened, as expected for any field-theoretic regulator, and the effect is only logarithmic in the Higgs mass so that the sensitivity is reduced considerably.

Nevertheless, from the "Blue-Band Plot", cf. Fig. 12, in which the set of all the established precision measurements is summarized, a most probable value of about 100 GeV is indicated, with large error though, for the Higgs mass in the Standard Model and related theories, such as supersymmetric theories. An upper bound close to 200 GeV has been found in the analysis [13]:

$$M_H = 91^{+58}_{-37}\ \text{GeV}$$
$$M_H < 202\ \text{GeV}$$

Thus, in the framework of the Standard Model and in a large class of potential extensions, LEP data point to a moderately small Higgs mass in the intermediate mass range of the particle. This is corroborated by analyses of all the individual observables except the forward–backward asymmetry of b jets. This indirect evidence for a light Higgs sector is complemented by indirect counter-evidence against a large class of models constructed for generating mechanisms of electroweak symmetry breaking by new strong interactions.

4.2 Real Higgs mass bound

The direct search for the Higgs particle in the Higgs-strahlung process $e^+e^- \to ZH$ has set a stringent lower limit on the mass of the particle in the Standard Model [32]:

$$M_H > 114.4\ \text{GeV} \quad [95\%\ \text{C.L.}]$$

However, we have been left with a 1σ effect for Higgs masses in excess of 115 GeV, fueled by the 4-jet channel in one experiment. "This deviation, although of low significance, is compatible with a Standard Model Higgs boson in this mass range while being also in agreement with the background hypothesis" [32].

5 Summary

Based on the high-precision measurements by the four experiments, ALEPH, DELPHI, L3 and OPAL, and in coherent action with a complex *corpus* of theoretical analyses, LEP led to an impressive set of fundamental results, the traces of which will be imprinted in the history of physics:

- Essential elements of the Standard Model of particle physics are firmly established at the quantum level:
  - the SU(3) × SU(2) × U(1) multiplet structure of the fundamental constituents of matter and their interactions with the strong and electroweak gauge bosons;
  - the gauge symmetry character of the self-interactions among the electroweak bosons $W^\pm, Z$ and γ, and among the gluons.
- Indirect evidence has been obtained for the existence of a light Higgs boson in Standard Model type scenarios.
- The extrapolation of the three gauge couplings points to the Grand Unification of the individual gauge interactions at a high energy scale – compatible with the supersymmetric extension of the Standard Model in the TeV range.

In the precision analyses performed at LEP, many physics scenarios beyond the Standard Model were probed, constraining their scale parameters to ranges between the upper LEP energy and the TeV and multi-TeV scales. These studies led to a large number of bounds on masses of supersymmetric particles, masses and mixings of novel heavy gauge bosons, scales of extra spacetime dimensions, radii of leptons and quarks, and many other examples.

In conclusion:
LEP has made significant contributions to the process of establishing the Standard Model for matter and forces.

In addition, experiments at LEP have built a platform for physics scenarios beyond the Standard Model in the TeV range which can shortly be explored at the hadron collider LHC under construction and prospective electron–positron linear colliders.

Acknowledgements. Special thanks for help in preparing this report go to S. Bethke, G. A. Blair, A. Brandenburg, K. Desch, M. Grünewald, W. Porod, and R. Seuster.

References

1. S.L. Glashow, Nucl. Phys. **22**, 579 (1961); A. Salam, in: Elementary Particle Theory, Stockholm 1969; S. Weinberg, Phys. Rev. Lett. **19**, 1264 (1967)
2. S. Weinberg, these Proceedings
3. P.W. Higgs, Phys. Rev. Lett. **13**, 508 (1964) and Phys. Rev. **145**, 1156 (1966); F. Englert, R. Brout, Phys. Rev. Lett. **13**, 321 (1964); G.S. Guralnik, C.R. Hagen, T.W.B. Kibble, Phys. Rev. Lett. **13**, 585 (1964); T.W.B. Kibble, Phys. Rev. **155**, 1554 (1967)
4. F.J. Hasert et al., [Gargamelle Collaboration], Phys. Lett. B **46**, 121 and 138 (1973)
5. D. Haidt, these Proceedings
6. G. Arnison et al., [UA1 Collaboration], Phys. Lett. B **122**, 103 (1983) and B **126**, 398 (1983); M. Banner et al. [UA2 Collaboration], Phys. Lett. B **122**, 476 (1983); P. Bagnaia et al. [UA2 Collaboration], Phys. Lett. B **129**, 130 (1983)
7. P. Darriulat, these Proceedings
8. G. 't Hooft, Nucl. Phys. B **33**, 173 (1971) and B **35**, 167 (1971); G. 't Hooft and M. Veltman, Nucl. Phys. B **44**, 189 (1972)
9. S.L. Glashow, J. Iliopoulos, L. Maiani, Phys. Rev. D **2**, 1285 (1970)
10. J. Ellis, these Proceedings
11. G. Altarelli, Proceedings, International Symposium on Lepton and Photon Interactions at High Energies, Stanford 1989
12. L. Camilleri, D. Cundy, P. Darriulat, J. Ellis, J. Field, H. Fischer, E. Gabathuler, M.K. Gaillard, H. Hoffmann, K. Johnson, E. Keil, F. Palmonari, G. Preparata, B. Richter, C. Rubbia, J. Steinberger, B. Wiik, W. Willis, K. Winter, Report CERN **76-18**, [8 November 1976]
13. LEP Electroweak Working Group, CERN-EP/2002-091[hep-ex/0212036] and updates on http://lepewwg.cern.ch/LEPEWWG/
14. D. Schaile and P.M. Zerwas, Phys. Rev. D **45**, 3262 (1992)
15. M. Veltman, Nucl. Phys. B **123**, 89 (1977)
16. D. Schaile, Proceedings, XXVII International Conference on High Energy Physics, Glasgow 1994
17. H. Fritzsch, M. Gell-Mann, Proceedings, XVI International Conference on High Energy Physics, Chicago-Batavia 1972
18. S. Bethke, Proceedings, International Conference on QCD, Montpellier 2002, and references therein
19. D.J. Gross, F. Wilczek, Phys. Rev. Lett. **30**, 1343 (1973); H.D. Politzer, Phys. Rev. Lett. **30**, 1346 (1973)
20. B. Adeva et al., [L3 Collaboration], Phys. Lett. B **248**, 227 (1990)
21. M. Bengtsson, P.M. Zerwas, Phys. Lett. B **208**, 306 (1988)
22. G. Abbiendi et al., [OPAL Collaboration], Eur. Phys. J. C **20**, 601 (2001)
23. W. Bernreuther, A. Brandenburg, P. Uwer, Phys. Rev. Lett. **79**, 189 (1997); G. Rodrigo, A. Santamaria, M.S. Bilenky, Phys. Rev. Lett. **79**, 193 (1997); P. Abreu et al., [DELPHI Collaboration], Phys. Lett. B **418**, 430 (1998); R. Barate et al., [ALEPH Collaboration], Eur. Phys. J. C **18**, 1 (2000); G. Abbiendi et al., [OPAL Collaboration], Eur. Phys. J. C **21**, 411 (2000)
24. H. Georgi, H. Quinn, S. Weinberg, Phys. Rev. Lett. **33**, 451 (1974)
25. S. Dimopoulos, S. Raby, F. Wilczek, Phys. Rev. D **24**, 1681 (1981); L.E. Ibanez, G.G. Ross, Phys. Lett. B **105**, 439 (1981); U. Amaldi, W. de Boer, H. Fürstenau, Phys. Lett. B **260**, 447 (1991); P. Langacker, M. Luo, Phys. Rev. D **44**, 817 (1991); J. Ellis, S. Kelley, D.V. Nanopoulos, Phys. Lett. B **260**, 161 (1991)
26. G.A. Blair, W. Porod, P.M. Zerwas, Eur. Phys. J. C **27**, 263 (2003)
27. H. Weyl, Z. Phys. **56**, 330 (1929)
28. C.N. Yang, R.L. Mills, Phys. Rev. **96**, 191 (1954)
29. W. Alles, C. Boyer, A. Buras, Nucl. Phys. B **119**, 125 (1977)
30. P. Wells, Proceedings, International Europhysics Conference on High Energy Physics, Aachen 2003
31. M. Veltman, Acta Phys. Polon. **B 8**, 475 (1977)
32. R. Barate et al., [LEP Higgs Working Group], Phys. Lett. B **565**, 61 (2003)